Journal of Power Sources 187 (2009) 605–612

Contents lists available at ScienceDirect

Journal of Power Sources

journal homepage: www.elsevier.com/locate/jpowsour

Application of ionic liquids as an electrolyte additive on the electrochemical behavior of lead acid battery

Behzad Rezaei*, Shadpour Mallakpour, Mahmood Taki

Department of Chemistry, Isfahan University of Technology, Isfahan 84156-83111 Islamic Republic of Iran

ARTICLE INFO

Article history:
Received 29 July 2008
Received in revised form
22 September 2008
Accepted 19 October 2008
Available online 5 November 2008

Keywords:
Lead acid battery
Ionic liquids
Electrolyte additives
Lead–antimony alloy
Hydrogen and oxygen overpotentials

ABSTRACT

Ionic liquids (ILs) belong to new branch of salts with unique properties which their applications have been increasing in electrochemical systems especially lithium-ion batteries. In the present work, for the first time, the effects of four ionic liquids as an electrolyte additive in battery's electrolyte were studied on the hydrogen and oxygen evolution overpotential and anodic layer formation on lead–antimony–tin grid alloy of lead acid battery. Cyclic and linear sweep voltammetric methods were used for this study in aqueous sulfuric acid solution. The morphology of grid surface after cyclic redox reaction was studied using scanning electron microscopy. The results show that most of added ionic liquids increase hydrogen overpotential and whereas they have no significant effect on oxygen overpotential. Furthermore ionic liquids increase antimony dissolution that might be related to interaction between Sb^{3+} and ionic liquids. Crystalline structure of $PbSO_4$ layer changed with presence of ionic liquids and larger $PbSO_4$ crystals were formed with some of them. These additives decrease the porosity of $PbSO_4$ perm selective membrane layer at the surface of electrode. Also cyclic voltammogram on carbon–PbO paste electrode shows that with the presence of ionic liquids, oxidation and reduction peak current intensively increased.

1. Introduction

During the last two decades the lead acid battery has been widely used in battery driven vehicles and for storing electrical energy from non-conventional sources. In spite of rapid improvement in its performance and design, there remain some problems of the battery which are yet to be solved [1]. One of these main problems is decomposition of water which led to hydrogen and oxygen evolution during overcharging. Gas evolution increases risk of explosion, corrosion of the grid alloys and water consumption. Also the electrolyte would be depleted prematurely and catastrophic failure would result [2]. In order to reduce water consumption in maintenance free batteries the hydrogen and oxygen evolution overpotentials must be increased by different strategies proposed in the literature [3–6]. The use of low-antimony or antimony-free alloys are effective ways to minimize gassing and to achieve maintenance-free lead acid batteries. The addition of Ca in the grid alloy increases its hardness. Considering the gassing processes the addition of Ca does not change substantially the hydrogen and oxygen overvoltage, i.e. the grid works as a pure lead one, where the oxygen and hydrogen overvoltages are the highest known. Considering the corrosion, the calcium can cause accelerated corrosion of the cast on strap connection in VRLA batteries, where this connection is exposed to gaseous oxygen, as well as accelerated positive grid corrosion [3,4]. Another solution which offers improvement of the battery is the use of additives in electrolyte and active materials. The additives should be stable in highly oxidation environment at high anodic potentials. The expander materials are commonly a mixture of inorganic and organic substances which act as dispersant agents by maintaining a highly porous active mass. They also exert other beneficial effects on the behavior of the negative plate by influencing the hydrogen overpotential and inhibiting the effects of impurities [5]. Among the electrolyte additives used so far the most widely investigated is H_3PO_4 [6,7] which has been reported as a beneficial additive in terms of improving cyclic life, decreasing self discharge and increasing the oxygen overpotential on the positive electrode. Other electrolyte additives, like H_3BO_3 [8], $SnSO_4$ [9] and sodium sulfate [10,11] are also prominent.

On the other hand, during the past decade, ionic liquids (ILs) have attracted the attention of many research groups in the field of energy storage [12]. ILs consist of large organic cations, such as quaternary ammonium cations [13], heterocyclic aromatic compounds [14], pyrrolidinium cations [15], with a variety of anions. The overall properties of ILs were dominated by cationic species including an alkyl chain or various functional groups and anionic species. Usually, in ILs, the anion controls their water miscibility

* Corresponding author. Tel.: +98 311 3913268; fax: +98 311 3912350.
E-mail addresses: rezaei@cc.iut.ac.ir, rezaeimeister@gmail.com (B. Rezaei).

0378-7753/$ – see front matter © 2008 Elsevier B.V. All rights reserved.
doi:10.1016/j.jpowsour.2008.10.081

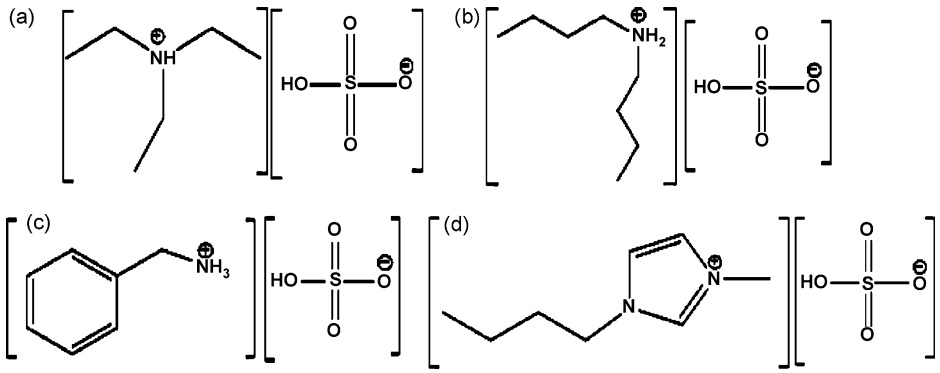

Scheme 1. Molecular structure of (a) triethyl ammonium hydrogen sulfate, (b) dibutyl ammonium hydrogen sulfate, (c) benzylammonium hydrogen sulfate, (d) 1-butyl-3-methylimidazolium hydrogen sulfate.

or ionic mobility, and the cation has an impact on their hydrophobicity, viscosity, density or melting point according to the physical nature or volume size of the cation and anion species [16]. However, this trend is not exactly consistent with all species of ILs and can be altered by a change of physical state caused by supplying the thermal energy into the ILs or a different interaction between cation and anion [17]. The combination of anionic and cationic species in ILs gives them a lot of variation in properties such as, treated as liquid at ambient temperature, thermal stability, nonflammability, high ion density, wide electrochemical windows and designable [18]. Because of these unique properties, ionic liquids can be applied in many electrochemical devices such as Li-ion batteries [12,19,20], super capacitors [21], solar cells [22] and fuel cells [23].

There are no reports about application of ILs on the electrical performance of lead acid batteries. In this work, effects of four different ionic liquids which are added to electrolyte, on the electrochemical properties of lead acid battery and especially on the polarization potentials of hydrogen and oxygen evolution gas are investigated using cyclic voltammetric method. The IUPAC name and structures of used ionic liquids are: triethyl ammonium hydrogen sulfate (Scheme 1(a)), dibutyl ammonium hydrogen sulfate (Scheme 1(b)), benzylammonium hydrogen sulfate (Scheme 1(c)) and 1-butyl-3-methylimidazolium hydrogen sulfate (Scheme 1(d)).

2. Experimental

2.1. Preparation of working electrodes

The iron mould with cooling system and temperature control unit as the same as grid casting machine of Sovema Co. was used for preparing of working electrode. The working electrodes which were used consist of seven lead antimony wires with different antimony percentages. The composition of the alloys was Pb–Sb–Sn (X%, Sb; 0.24%, Sn) where X = 0.32, 0.50, 0.73, 1.66, 1.88, 2.50, 2.80 wt.%. The sides and other parts of the working electrodes were covered with an epoxy resin to avoid any contact with electrolyte solution, except electrode surface exposing a 0.50 cm^2 surface area of the alloy.

Carbon–lead oxide paste electrodes were prepared as follows: 0.20 g of graphite powder, which was washed with ethanol and dried under vacuum, was added to 0.20 g PbO powder and mixed with 0.1 cm^3 of Nujol mall. This paste was transferred into a glass tube with 0.50 cm^2 diameter and pressed to obtain compact structure that its electrical resistance is below 10.0 Ω. Finally the electrode tip was polished with smooth paper.

2.2. Materials and electrolytes

All of ILs which are used in this study have been synthesized and purified in our polymer laboratory. Sulfuric acid, graphite powder and lead oxide were reagent grade (from Merck) and deionized doubly distilled water was used for the preparation of all solutions. The electrolyte was 4.0 mol dm^{-3} sulfuric acid (normal concentration of sulfuric acid in lead acid battery) which is prepared from concentrated H_2SO_4 and double distilled water. Electrolyte solutions contain 2.5, 5.0, 10.0, 15.0 and 20.0 mg cm^{-3} of each ionic liquid were prepared by adding known amount of ILs salts to the electrolyte.

2.3. Cyclic voltammetry measurements

The cyclic and linear sweep voltammograms (LSV) were obtained at a sweep rate 50.0 mV s^{-1}, in the potential range between hydrogen and oxygen evolution (−2.500 V to +2.500 V vs. saturated calomel electrode (SCE)) using a potentiostat–galvanostat of Behpajooh Co. Model BHP-2061-C connected to a personal computer. Working electrode was Pb–Sb–Sn alloy with different antimony contents. The counter and reference electrodes were platinum black and SCE, respectively. At the beginning of each experiment, the electrode was mechanically polished with water-resistant emery paper and washed with acetone and double distilled water. The cyclic voltammograms (CV) of carbon–lead oxide paste electrode, which is used as working electrode, were obtained at the sweep rate 50.0 mV s^{-1}, in the potential range of −0.600 to 1.000 V vs. SCE. The counter and reference electrodes were also platinum black and SCE, respectively.

2.4. SEM imaging

After one cycle of charge and discharge on the lead alloy electrodes, the SEM technique (Philips-XL30) was applied to studies the microstructures of surface layer. Because, the morphology of surface layer must be unchanged and epoxy resin is electrically insulator, a thin layer of Au was deposited on the electrodes before taking SEM imaging.

2.5. Tafel polarization measurement

For evaluation of the effects of these ILs on the corrosion rate of the alloy, LSV and tafel polarization measurement were carried out in a 4.0 mol dm^{-3} H_2SO_4 solutions with and without additives. The open circuit potential (E_{oc}) was determined by immersing Pb–Sb–Sn electrodes and SCE as a working and reference electrode in a 4.0 mol dm^{-3} H_2SO_4 solution. Then measuring of different potential was performed after the potential of the specimen becomes stable for a few minutes using a multimeter. For obtaining tafel plots, the potential was scanned at a rate of 10.0 mV s^{-1} in the cathodic direction between E_{oc} and E_{oc} −350.0 mV, and then in the

anodic direction between E_{oc} and E_{oc} +350.0 mV. All experiments were carried out at room temperature (298 K).

3. Results and discussion

Fig. 1 shows a CV recorded on a lead–1.6% antimony electrode in 4.0 mol dm^{-3} H_2SO_4 solution in the potential region between hydrogen and oxygen evolution (from −2.500 V to +2.500 V vs. SCE). According to the literatures [24,25] peaks H and O are assigned to reduction of hydrogen ions and oxidation of water that led to hydrogen and oxygen evolution, respectively. During the anodic potential sweep of the voltammogram, the current peak A_1, corresponding to the formation of lead sulfate [26–29] was recorded and the oxidation current peak A_2 at a potential of about 0.00 V is related to the oxidation of antimony in electrode alloy [30]. In the cathodic potential sweep, five current peaks appeared, corresponding to the transitions of PbO_2 to $PbSO_4$ (C_5) [31–33], PbO to Pb (C_3) [34–36] and $PbSO_4$ to Pb (C_1,C_2) [25,26–29]. The small reduction current peak C_4 at a potential of about −0.25 V is related to the reduction of antimony and its species [30]. Two reduction peaks of $PbSO_4$ appear clearly on the negative going potential sweep curves (C_1 and C_2). They represent the reduction of $PbSO_4$ crystals with different sizes. The more negative reduction peak (C_1) is the reduction of the big $PbSO_4$ crystals. In charge/discharge cycles, many small $PbSO_4$ crystals are formed over the big crystals which are very difficult to be reduced [37]. The electrode surface is covered by many small $PbSO_4$ crystals. The anodic layer formed in the region between −0.52 and 0.00 V vs. SCE, which is composed of lead(II) sulfate crystals, passivates the electrode surface. The wide current plateau above 0.00 V, where the current is independent of the potential, corresponds to the potential region in which lead oxide formation occurs, with the (+2) oxidation state of lead. Since the PbO layer is in a direct contact with the electrode, its reduction is possible, which results in the current peak C_3 in the cathodic portion of the voltammogram. Results of some investigations indicate that lead oxidation to PbO or basic sulfates under the $PbSO_4$ membrane begin at potential of −0.20 V vs. SCE [38,39]. The initial reaction of sulfuric acid with lead oxide, gives normal lead sulfate and heat evolution. Under the influence of excess lead oxide and water, this is not stable, so converts into basic lead sulfate, either tribasic lead sulfate ($3PbO{\cdot}PbSO_4$) or tetrabasic lead sulfate ($4PbO{\cdot}PbSO_4$). Tribasic lead sulfate is crystallized as small needles with high specific surface, however; tetrabasic lead sulfate forms more bulky crystals.

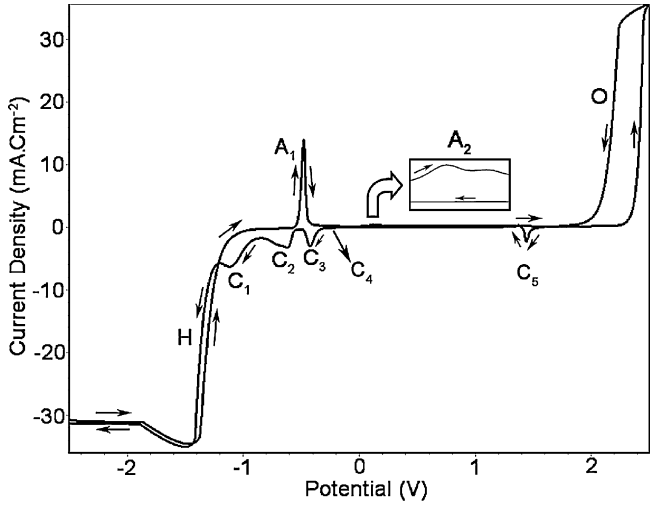

Fig. 1. Cyclic voltammogram of Pb–1.6%Sb–0.24% Sn alloy at the scan rate of 50 mV s^{-1} in 4.0 mol dm^{-3} H_2SO_4.

The oxidation of antimony begins at the PbO formation potential within a semi permeable $PbSO_4$ membrane. With an increase in antimony content in the alloy the current peak height (A_2) increases. With respect to the corresponding cathodic current peak C_2, may be explained by the formation of soluble antimony species, which leave the electrode by passing through the pores on the $PbSO_4$ membrane. The passivation current also increases with increasing antimony content in the lead alloy, which points to greater porosity of the sulfate membrane. Porosity retards the increase in pH values inside the sulfate membrane on the Pb–Sb electrode, with respect to the membrane formed under the same conditions on the Pb electrode. This is probably the reason why the amount of PbO formed during oxidation of the Pb–Sb electrode is smaller than in the case of Pb oxidation. The water loss in the batteries with positive grids cast from Pb–Sb–Sn alloys is high, because antimony from the positive grid can migrate through the electrolyte and be deposited on the surface of the negative plate, where it diminish the overpotential for hydrogen evolution [40]. For this reason, in maintenance free battery, the grid was made with low antimony alloy (1–2 wt.%). Therefore in this study, most of experiments were carried out on the Pb–1.6% Sb alloy. It is interesting to note that, in the anodic portion of the cycle after the potential region in which lead(II) compounds form, the current peak corresponding to the formation of a PbO_2 layer (E_{red} (PbO_2/$PbSO_4$) = 1.38 V) does not appear. An increase in the anodic current at $E > 1.70$ V occurs due to oxygen evolution at the electronically conducting β-PbO_2 phase [31,41,42]. A hysteresis is also observed, which is explained by the connection between the overpotential of β-PbO_2 formation and overpotential of oxygen evolution. In the anodic potential sweep, the overpotential of β-PbO_2 nucleation is the limiting factor in the oxygen evolution reaction. In the cathodic potential sweep, since the β-PbO_2 phase at the surface of the electrode is already formed, oxygen evolution takes place at a lower overpotential. Sharpe [31,41] has noticed that the presence of antimony in a lead alloy inhibits the formation of β-PbO_2 and facilitates the formation of α-PbO_2.

In this study, each of the ILs was added to the electrolyte in different concentrations and their electrochemical behavior changes were investigated especially on the hydrogen and oxygen evolution overpotential and electrode passivation in sulfuric acid solution. Hydrogen sulfate is a common ion so the effects of added IL, is because of cationic species in electrolyte. Interaction between this cations and charged species in electrolyte, change the structures of basic lead sulfate formed on the surface electrode and other electrochemical behaviors changes would be observed.

3.1. Hydrogen evolution potential

Fig. 2 shows LSV of Pb–1.6% Sb–0.24% Sn alloy in negative potential direction scanning for various IL with equal concentrations (2.5 mg cm^{-3}) in 4.0 mol dm^{-3} sulfuric acid electrolyte. According to this figure, within added triethyl ammonium hydrogen sulfate lowers absolute hydrogen overpotential and other added compounds shift it to more negative potentials. Dibutyl ammonium hydrogen sulfate has the most effective additives. In order to consider IL concentration on hydrogen overpotential, this potential was obtained at the current density of −30.0 mA cm^{-2} in LSV indicated in Fig. 2 and depicted in Fig. 3. As can be seen in Fig. 3, except triethyl ammonium hydrogen sulfate that shows irregular behavior, with increased IL concentration, hydrogen overpotential shifts to more negative value. Antimony has catalytic effect on the hydrogen evolution potential which was mentioned previously. In order to study the effect of ILs on this catalytic behavior (at the same concentration), hydrogen reduction potential at the current density of −30.0 mA cm^{-2} which was obtained via LSV at different

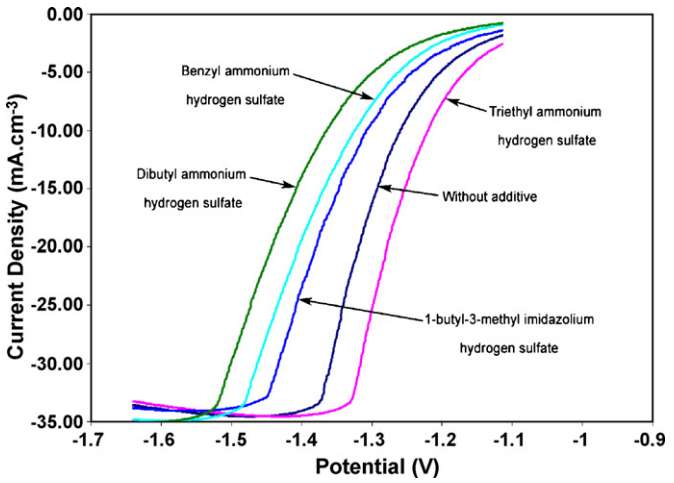

Fig. 2. Linear sweep voltammograms of Pb–1.6%Sb–0.24% Sn alloy at the scan rate of 50 mV s^{-1} in 4.0 mol dm^{-3} H_2SO_4 with various ionic liquid with equal concentrations (2.5 mg cm^{-3}).

antimony concentration in working electrode and the results are shown in Fig. 4. The obtained results show that although IL additives increase absolute hydrogen potential, but, they would not eliminate antimony catalytic effect. Therefore it has been seen from Fig. 4 that despite ILs increase absolute hydrogen evolution potential, with increased antimony percent in the alloy, this potential decreased similar to solution without additive. Considering that, working electrodes and other experiment conditions (like temperature and pressure) are alike and according to the Nernst equation, shifting hydrogen overpotential to more negative values related to decrease hydrogen ion concentration in beneath $PbSO_4$ perm selective membrane. Consequently ILs in electrolyte unlike antimony, decreases the porosity of $PbSO_4$ perm selective membrane.

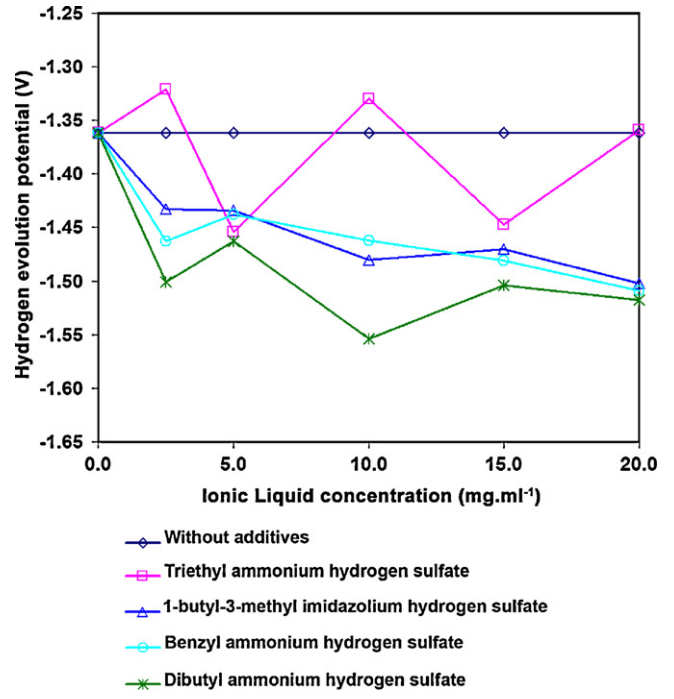

Fig. 3. Hydrogen reduction potentials in different ionic liquid concentrations at the current density of −30.0 mA cm^{-2} in linear sweep voltammograms using Pb–1.6%Sb–0.24% Sn as working electrode and the scan rate of 50 mV s^{-1} in 4.0 mol dm^{-3} H_2SO_4.

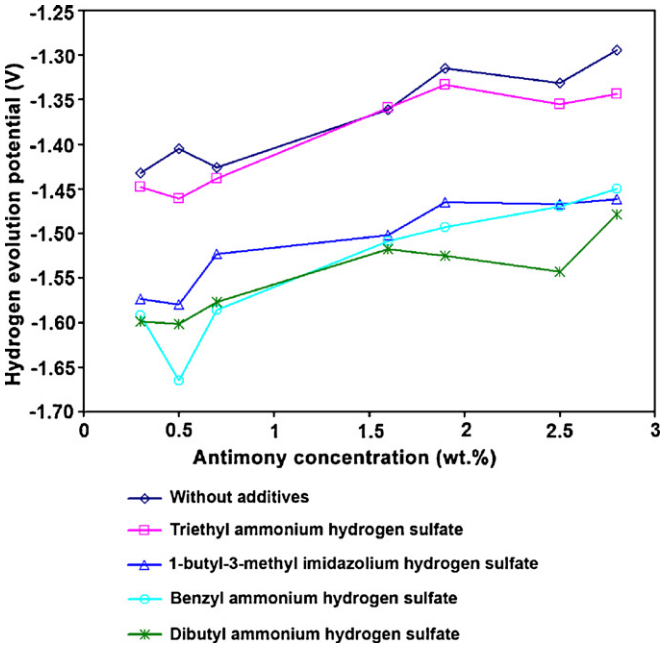

Fig. 4. Hydrogen reduction potential at the current density of −30.0 mA cm^{-2} versus antimony concentration in four electrolytes contains 4.0 mol dm^{-3} H_2SO_4 and 20.0 mg cm^{-3} of each ionic liquid. (Scan rate in Linear sweep voltammograms: 50 mV s^{-1}).

3.2. Oxygen evolution potential

The effect of concentration of added ILs in the range of 2.5–20.0 mg cm^{-3} on oxygen overpotential shows in Fig. 5. Oxygen reduction potential was obtained at the current density of 30.0 mA cm^{-2} in LSV. The results indicate that, only 1-butyl-3-methylimidazolium hydrogen sulfate seriously increased oxygen

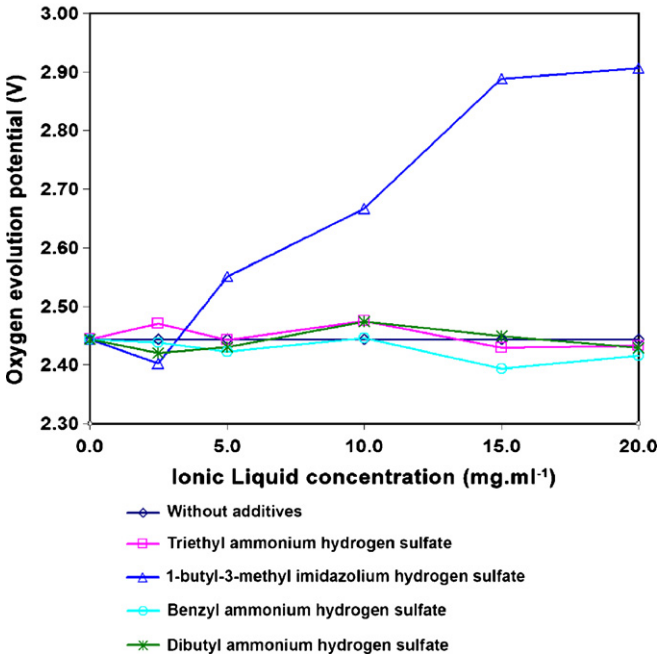

Fig. 5. Oxygen evolution potential at the current density of 30.0 mA cm^{-2} in different ionic liquid concentrations at the current density of 30.0 mA cm^{-2} in linear sweep voltammograms using Pb–1.6%Sb–0.24% Sn as working electrode and the scan rate of 50 mV s^{-1} in 4.0 mol dm^{-3} H_2SO_4.

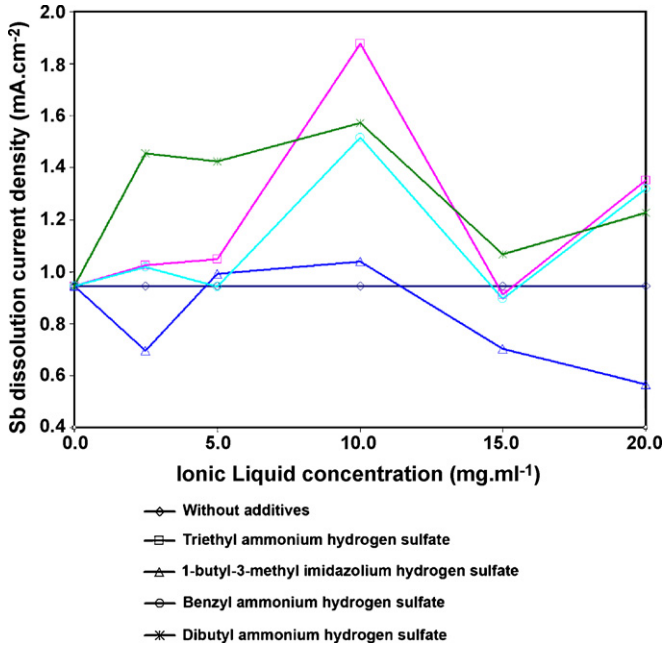

Fig. 6. Effect of ionic liquid additives on antimony dissolution using Pb–2.8%Sb–0.24% Sn as working electrode and the scan rate of 50 mV s^{-1} in 4.0 mol dm^{-3} H_2SO_4.

reduction potential. Oxygen evolution potential depends on the film characteristics, because it takes place on the PbO_2 film, thus we observed other added compounds have no significant effect on this potential. As it was mentioned previously, β-PbO_2 formation and oxygen evolution occur at high anodic potentials. It seems that 1-butyl-3-methylimidazolium hydrogen sulfate increases β-PbO_2 nucleation potential. With increase in hydrogen and oxygen overpotential with ILs as electrolyte additives, water decomposition and consumption will be decreased.

3.3. Antimony dissolution

Antimony oxidation current (peak A_2 in Fig. 1) used in order to consider antimony dissolution in electrolyte with and without ILs additives. Fig. 6 shows antimony current density for different concentration of ILs additives. All experiments were performed using Pb–2.8% Sb–0.24% Sn as working electrode. The results show ILs may cause increased antimony dissolution rate. This effect might be related to interaction between Sb^{3+} and ILs that makes more stable species containing Sb^{3+} ion which increase antimony current density.

3.4. Formation and reduction of oxide layer on Pb–Sb electrode surface

Fig. 7 shows CV in solutions with and without each of the ILs additives. These additives in electrolyte cause different effects in the CV curves. The oxidation current of Pb to $PbSO_4$ (peak A_1 in Fig. 7) related to the formation of lead sulfate crystals increases with the addition of triethyl ammonium hydrogen sulfate and 1-butyl-3-methylimidazolium hydrogen sulfate. Consequently reduction peak of $PbSO_4$ (Peak C_1 and C_2 in Fig. 7a and b) was also increased. Current peak C_1 in Fig. 7a and b that is related to the reduction of large $PbSO_4$ crystals seriously increased with triethyl ammonium hydrogen sulfate and 1-butyl-3-methylimidazolium hydrogen sulfate in electrolyte. It means that larger $PbSO_4$ crystals have been formed in the presence of these additives. Fig. 8a and b demonstrate

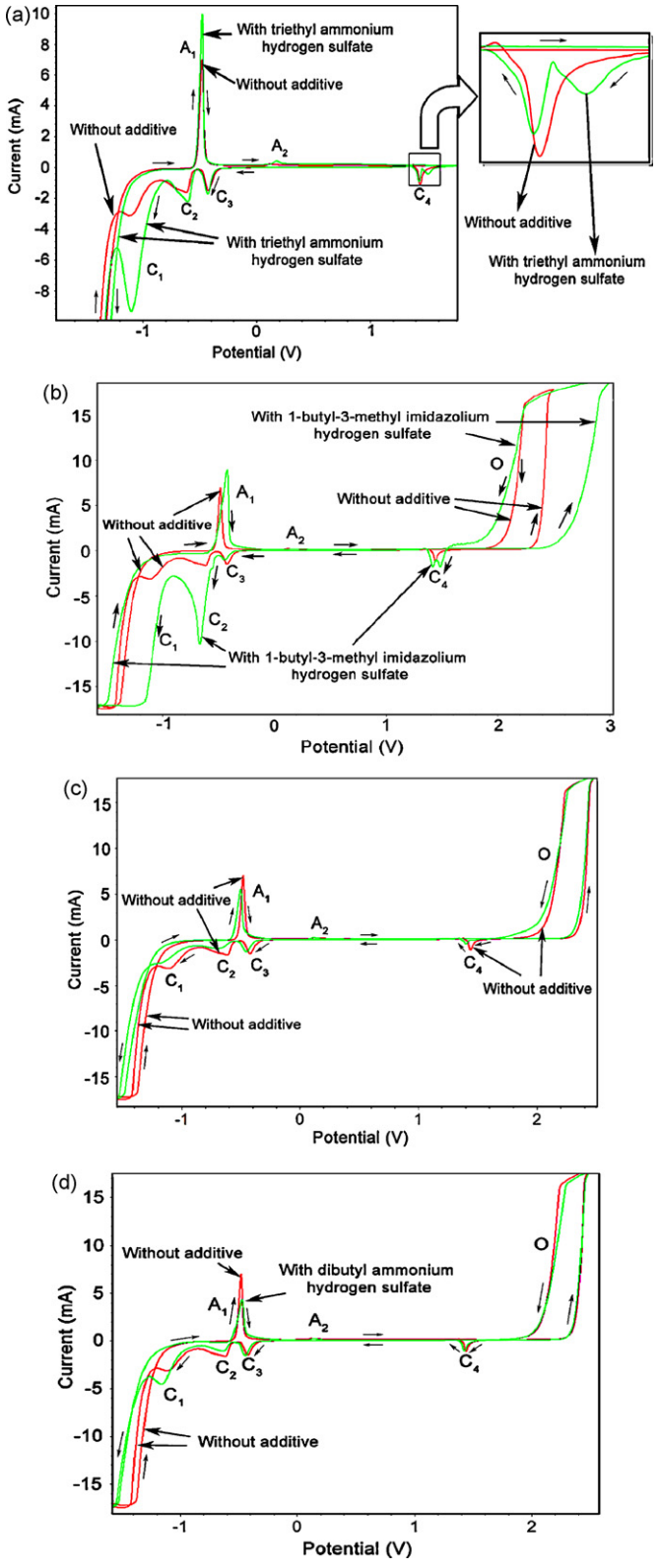

Fig. 7. Cyclic voltammograms in solution with and without ionic liquid additive. (a) 2.5 mg cm^{-3} of triethyl ammonium hydrogen sulfate; (b) 15 mg cm^{-3} of 1-butyl-3-methylimidazolium hydrogen sulfate; (c) 2.5 mg cm^{-3} of benzylammonium hydrogen sulfate and (d) 15 mg cm^{-3} dibutylammonium hydrogen sulfate. All cyclic voltammograms were obtained using Pb–1.6%Sb–0.24%Sn as working electrode and the scan rate of 50 mV s^{-1} in 4.0 mol dm^{-3} H_2SO_4.

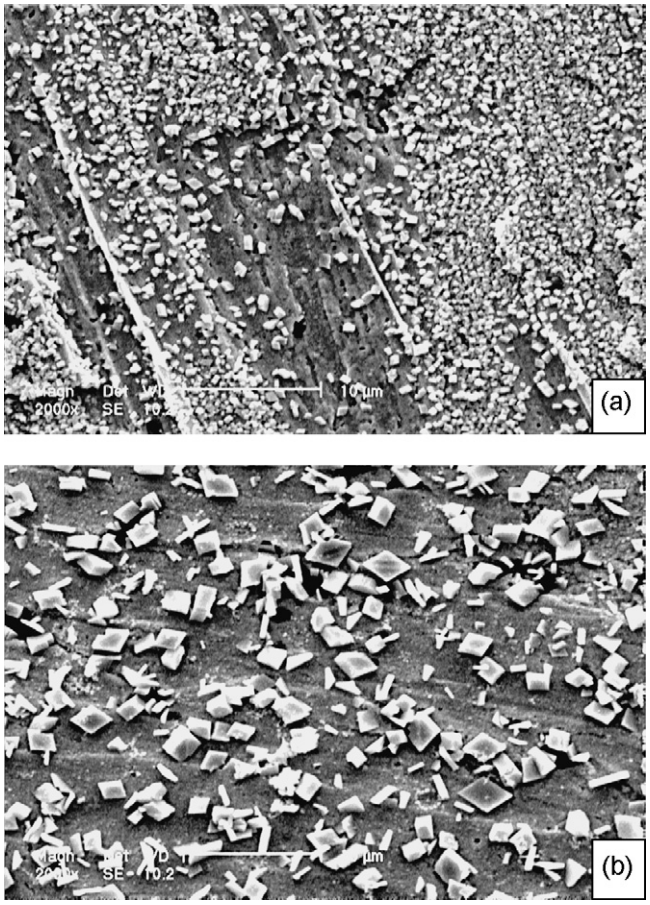

Fig. 8. The scanning electron micrographs (SEM) after using one cycle of charge and discharge for Pb–1.6%–Sb–0.24%Sn alloy in 4.0 mol dm^{-3} H_2SO_4. (a) without additive; (b) with 5.0 mg cm^{-3} 1-butyl-3-methylimidazolium hydrogen sulfate.

the SEM of the lead–antimony electrodes after using one cycle of charge and discharge in sulfuric acid solution with and without 1-butyl-3-methylimidazolium hydrogen sulfate. The results show that: (i) the crystals that formed on lead alloy in solution with this IL are larger in size than those on electrolyte without additive. The average diameter of crystals formed on solution without this additive is 0.82 μm however, in electrolyte with additive; the average diameter size is 3.24 μm that approves the results obtained from CV. (ii) The distribution of $PbSO_4$ crystals showed in Fig. 8b are uniform and similar to tetrabasic lead sulfate structure which have low specific surface and cover small surface area of the electrode. Consequently larger surface area exposed to the electrolyte that might increase grid corrosion. Reduction peaks C_4 which are related to reduction of PbO_2 to $PbSO_4$ changed with ILs. In solution with triethyl ammonium hydrogen sulfate and 1-butyl-3-methylimidazolium hydrogen sulfate this peak splits to two peaks. This is because of the formation of more β-PbO_2 in the presence of ILs that reduce in greater potentials toward α-PbO_2. In Fig. 7b a large hysteresis observed in peak O that is related to the formation of β-PbO_2 which reduced in peak C_4. In benzylammonium hydrogen sulfate solution fewer and smaller $PbSO_4$ crystals were formed.

3.5. Positive and negative active material

During discharge and charge process in lead acid batteries Pb in negative electrode and PbO_2 in positive electrode changed to Pb (II) and vice versa. According to previous statements, PbO in H_2SO_4 solution reacts immediately with the acid forming lead sulfate and basic lead sulfates (tribasic or tetrabasic). The electrochemical effects of ILs in conversion of $PbSO_4$ to PbO_2 and vice versa were investigated by carbon/PbO electrode. CV of the paste electrode in solution with benzylammonium hydrogen sulfate in the potential range between Pb (II) oxidation and reduction has been shown in Fig. 9. Other ILs have similar voltammograms. According to this figure, potential and current of reduction and oxidation peaks increased with benzylammonium hydrogen sulfate. Fig. 10 shows current peak $PbSO_4$ to PbO_2 and E_{pa}–E_{pc} versus ILs concentrations. The results indicate that addition of these ILs to the battery electrolyte, increase current conversion of $PbSO_4$ to PbO_2. Interaction between Pb^{2+} and ILs, make more stable species of Pb^{2+}. Therefore, more $PbSO_4$ formed which led to increase current conversion of $PbSO_4$ to PbO_2 that is beneficial effect in negative and positive active material in the battery. However from Fig. 10b all of added compounds increase peak potential difference. In another words electrochemical processes with ILs become more irreversible.

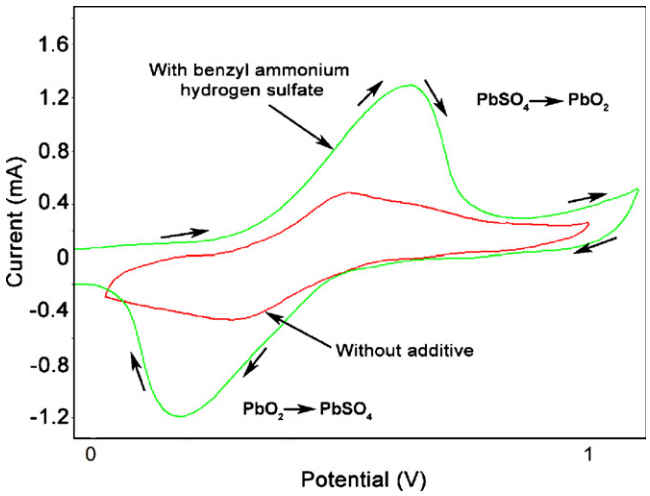

Fig. 9. Cyclic voltammogram of carbon/PbO paste electrode in 4.0 mol dm^{-3} H_2SO_4 with and without 20.0 mg cm^{-3} benzylammonium hydrogen sulfate (ν = 50.0 mV s^{-1}).

3.6. Corrosion tests

There are two types of corrosion processes in the lead acid batteries. In the potential domain of the negative plate usually the cast on strap connection is vulnerable to the type of corrosion studied in the present work. But in the positive plate the anodic corrosion takes place via solid state mechanism – the evolution of the oxygen causes the penetration of oxygen atoms and anions in the crystal lattice of the lead, and PbO, PbOn and alpha PbO_2 are formed consecutively. The effects of these additives on grid corrosion rate have been considered using tafel polarization method. I_{corr} and E_{corr} are corrosion current density (μA cm^{-2}) and corrosion potential (V) obtained by extrapolation of cathodic and anodic tafel lines in solution with and without IL additives, respectively. With following equation, corrosion current density converted to corrosion rate: corrosion rate [mils per year (mpy)] = 0.129 (ai_{corr}/nD). Where a, is atomic weight of alloy (g mol^{-1}), D is density of alloy (g cm^{-3}), and n is the number of electrons participated in corrosion reaction [43]. Corresponding corrosion data are given in Table 1. These results show that IL additives increase grid corrosion. As anticipated previously, within added compounds 1-butyl-3-methylimidazolium hydrogen sulfate has the most effect on increasing of grid corrosion rate.

Table 1
Corrosion data for Pb–1.6% Sb alloy in 4.0 mol dm^{-3} H_2SO_4 in presence and absence of each ionic liquid additive obtained from tafel polarization method.

Ionic liquid (with hydrogen sulfate anion)	2.5 mg cm^{-3}			10.0 mg cm^{-3}			20.0 mg cm^{-3}		
	E_{corr} (V)	i_{corr} (μA cm^{-2})	mpy	E_{corr} (V)	i_{corr} (μA cm^{-2})	mpy	E_{corr} (V)	i_{corr} (μA cm^{-2})	mpy
Triethyl ammonium	−0.592	63.1	73	−0.581	85.3	99	−0.856	62.1	72
1-butyl-3-methylimidazolium	−0.587	137.1	160	−0.555	141.2	165	−0.564	112.2	131
Benzylammonium	−0.608	63.1	73	−0.592	82.4	96	−0.596	69.2	81
Dibutyl ammonium	−0.606	85.1	99	−0.588	79.4	92	−0.583	125.9	146
Without Ionic liquid	E_{corr} = −0.580, i_{corr} = 57.1 μA cm^{-2}, mpy = 67								

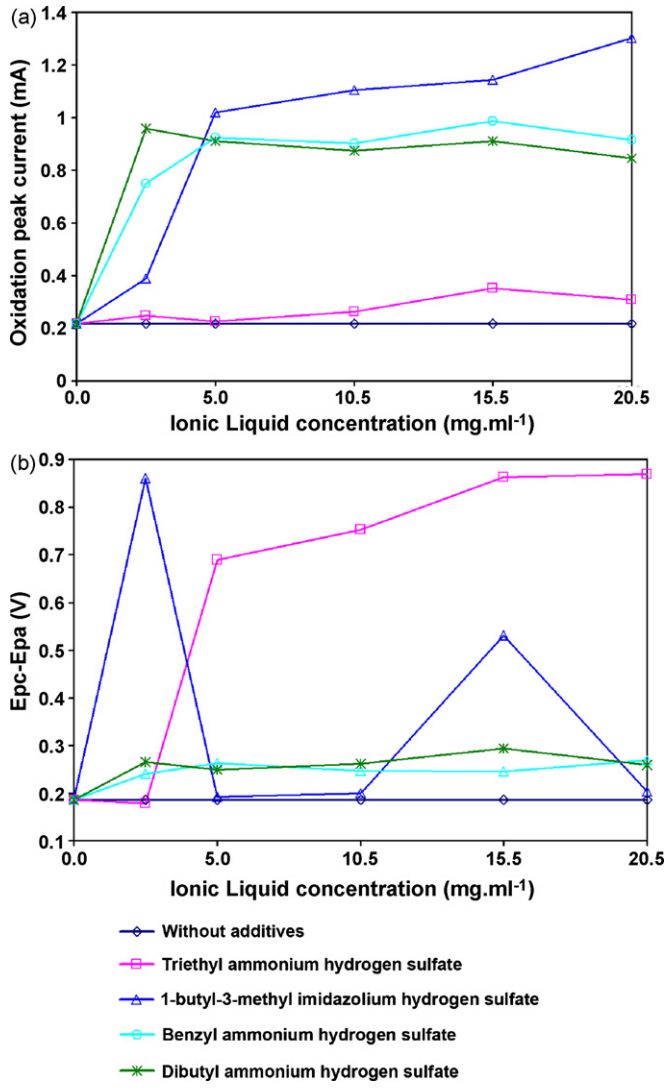

Fig. 10. Oxidation peak current (a) and peak potential difference (reversibility); (b) according to Ionic liquids concentrations.

4. Conclusion

In this study, the effects of ILs as an electrolyte additive were investigated on the electrochemical properties of lead acid battery. This investigation was performed by means of CV and SEM. The obtained results indicate the effect of ILs on the surface characteristics of lead–antimony electrode and polarization potential of hydrogen and oxygen gas evolution. The electrochemical behaviors of electrodes depend on ILs concentration in the electrolyte solution. With increase hydrogen and oxygen overpotential with ILs as electrolyte additives, water decomposition will be decreased. Also ILs increase the rate of the conversion of $PbSO_4$ to PbO_2, and vice versa, i.e. the addition of ILs can increase the utilization of the positive active material. The corrosion results show that IL additives increase grid corrosion rate. Generally ILs that have similar structures, cause similar effects on electrochemical behavior of the electrodes.

Acknowledgements

The authors acknowledge the Isfahan University of Technology Council and Center of Excellency in Sensor and Green Chemistry for supporting this work.

References

[1] A. Bhattacharya, I.N. Basumallick, J. Power Sources 113 (2003) 382–387.
[2] T.R. Crompton, Battery Reference Book, vol. 18, 3rd ed., Reed, Oxford, 2000, p. 5.
[3] N. Bui, P. Mattesco, P. Simon, J. Steinmetz, E. Rocca, J. Power Sources 67 (1997) 61–67.
[4] S.G. Hibbins, F.A. Timpano, D.J. Zuliani, US Patent no. 5 (1996), pp. 547–634.
[5] C. Francia, M. Maja, P. Spinelli, J. Power Sources 95 (2001) 119–124.
[6] D. Pavlov, J. Power Sources 42 (1993) 345–363.
[7] J. Garche, H. Doring, K. Wiesener, J. Power Sources 33 (1991) 213–220.
[8] W.A. Badawy, S.S. El-Egamy, J. Power Sources 55 (1995) 11–17.
[9] E. Voss, U. Hullmeine, A. Winsel, J. Power Sources 30 (1990) 33–40.
[10] A.L. Ferreira, J. Power Sources 95 (2001) 255–263.
[11] M.J. Weighall, J. Power Sources 116 (2003) 219–231.
[12] E. Markevich, V. Baranchugov, D. Aurbach, Electrochem. Commun. 8 (2006) 1331–1334.
[13] C.F. Poole, B.R. Kersten, S.S.J. Ho, M.E. Coddens, K.G. Furton, J. Chromatogr. 352 (1986) 407.
[14] V.R. Koch, C. Nanjundiah, R.T. Carlin, World Pat. 970 (1997) 2252.
[15] D.R. MacFarlane, P. Meakin, J. Sun, N. Amini, M. Forsyth, J. Phys. Chem. B 103 (1999) 4164.
[16] J.G. Huddleston, A.E. Visser, W.M. Reichert, H.D. Willauer, G.A. Broker, R.D. Rogers, Green Chem. 3 (2001) 156.
[17] A.B. McEwen, H.L. Ngo, K. LeCompte, J.L. Goldman, J. Electrochem. Soc. 146 (5) (1999) 1687.
[18] H. Ohno, Electrochemical Aspects of Ionic Liquids, Wiley, New York, 2005.
[19] H. Sakaebe, H. Matsumoto, K. Tatsumi, Electrochim. Acta 53 (2007) 1048–1054.
[20] M. Ishikawa, T. Sugimoto, M. Kikuta, E. Ishiko, M. Kono, J. Power Sources 162 (2006) 658–662.
[21] A. Balducci, U. Bardi, S. Caporali, M. Mastragostino, F. Soavi, Electrochem. Commun. 6 (2004) 566–570.
[22] Q. Dai, D.B. Menzies, D.R. MacFarlane, S.R. Batten, S. Forsyth, L. Spiccia, Y.B. Cheng, M. Forsyth, C. R. Chimie 9 (2006) 617.
[23] R.F. De Souza, J.C. Padilha, R.S. Goncalves, J. Dupont, Electrochem. Commun. 5 (2003) 728–731.
[24] T. Hirasawa, K. Sasaki, M. Taguchi, H. Kanecho, J. Power Sources 85 (2000) 44.
[25] R. Babic, M. Melikos-Hukoric, N. Lajqy, S. Brinic, J. Power Sources 52 (1994) 17.
[26] F. Caldara, A. Delmastro, G. Fracchia, M. Maja, J. Electrochem. Soc 127 (1980 1869).
[27] K.R. Bullock, G.M. Trischan, R.G. Burrow, J. Electrochem. Soc. 134 (1987) 1283.
[28] M.N.C. Ijomah, J. Electrochem. Soc. 134 (1987) 2960.
[29] E. Hamenoja, T. Laitinen, G. Sundholm, A. Yli Pentti, Electrochim. Acta 34 (1989) 233.
[30] M. Metikoš-Hukoviïc, R. Babiïc, S. Omanoviïc, J. Electroanal. Chem. 374 (1994) 199.
[31] T.F. Sharpe, J. Electrochem. Soc. 122 (1975) 845.
[32] K.R. Bullock, T.F. Sharpe, J. Electrochem. Soc. 126 (1979) 360.
[33] B.K. Mahato, W.H. Tiedemann, J. Electrochem. Soc. 130 (1983) 2139.
[34] Y. Guo, J. Electrochem. Soc. 143 (1996) 1157.
[35] Y. Guo, Electrochim. Acta 37 (1992) 495.
[36] R.G. Barradas, D.S. Nadezhdin, Can. J. Chem. 62 (1984) 596.
[37] Y. Guo, M. Wu, S. Hua, J. Power Sources 64 (1997) 65.
[38] S. Briníc, M. Metikoš-Hukovíc, R. Babíc, J. Power Sources 55 (1995) 19.

[39] Y. Guo, J. Electrochem. Soc. 138 (1991) 1222.
[40] A.I. Rusin, Modern Technology of Lead-Acid Batteries, Energiya Leningrad, 1987, p. 182.
[41] T.F. Sharpe, J. Electochem. Soc. 124 (1977) 168.
[42] A. Czerwinski, M. Zelazowska, M. Grden, K. Kuc, J.D. Milewski, A. Nowacki, M. Gwojci, Kopczyk, J. Power Sources 85 (2000) 49.
[43] M.G. Fontana, Corrosion Engineering, 3rd ed., McGraw-Hill Book Company, New York, 1985.